

Adsorbate-Induced Surface Stress: Phonon Anomaly and Reconstruction on Ni(001) Surfaces

J. E. Müller

Arbeitsgruppe für Schichten- und Ionentechnik, Kernforschungsanlage Jülich, D-5170 Jülich, Federal Republic of Germany

and

M. Wuttig and H. Ibach

Institut für Grenzflächenforschung und Vakuumphysik, Kernforschungsanlage Jülich, D-5170 Jülich, Federal Republic of Germany

(Received 26 February 1986)

Ab initio all-electron calculations for carbon and oxygen chemisorbed on nickel clusters indicate that the charge redistribution induced by the adsorbate causes repulsive stresses between the metal surface atoms. Using lattice-dynamics calculations we show that these stresses can account for the observed S_4 -phonon anomaly with $c(2 \times 2)$ oxygen overlayers, and also explain the carbon-induced surface reconstruction, via a softening of the A_2 mode at \bar{X} . The reconstruction has also been reproduced directly by total-energy calculations with use of a suitable cluster.

PACS numbers: 68.35.Ja, 68.35.Rh

Atomic chemisorption of carbon and oxygen on metal surfaces are representative examples of strongly bonding systems, i.e., systems in which binding energies are large compared with typical metal-metal interactions. Strong bonding necessarily implies major perturbations in the local electronic structure of the substrate, such as substantial changes in the metal pair interactions and/or the introduction of internal stresses in the substrate. Adsorbate-induced effects on the structure and dynamics of the Ni(001) surface have been studied experimentally and theoretically.¹⁻⁴ Of special interest in the present context is the anomalously low frequency of the S_4 phonon (Rayleigh wave) when the surface is covered with a $c(2 \times 2)$ overlayer of oxygen, and the reconstruction of the Ni(001) surface upon carbon chemisorption.¹ The reconstructed surface is schematically represented in Fig. 1(b). This structure derives from the unreconstructed one [Fig. 1(a)] through a rotation of the surface Ni atoms about the C atom to which they are bonded (notice that the environments of neighboring C atoms rotate in opposite directions). The same reconstruction has been recently observed for nitrogen chemisorption.⁵ Group-theoretical analysis of the vibrational eigenmodes of (001) surfaces with $c(2 \times 2)$ overlayers shows that the reconstruction pattern is equivalent to a frozen A_2 -type phonon at the \bar{X} point of the surface Brillouin zone.^{6,7} This led to the suggestion that the reconstruction and the anomalously low S_4 frequency for the oxygen-covered surface are likely to have a common origin. It has been proposed that this common origin could be either a weakening of the restoring forces which couple the surface Ni atoms to the second metal layer,⁷ or an attractive interaction of the adsorbate atom (adatom) with the second-layer Ni atom underneath together with a repulsive interaction to the Ni atoms of the first layer.⁸

In this Letter we demonstrate that neither of these models is supported by *ab initio* calculations of the electronic structure. The calculations show that the strong adatom-nickel bonds remove charge from the first nearest-neighbor Ni—Ni bonds between the atoms of the first metal layer. As a result, these bonds are not able to balance the repulsive interaction between the incompletely screened nuclei, leading to finite interatomic forces or stresses between the surface atoms. In a lattice-dynamical model with pairwise potentials, this corresponds to a nonzero first derivative of the pair potential between the surface atoms. We show that both effects, i.e., the softening of the A_2 mode (and thus the reconstruction) and the decrease of the frequency of the Rayleigh wave, are reproduced by this model. The reconstruction is also reproduced directly by total-energy calculations on a cluster of suitable geometry.

● Carbon — C-Ni bonds
○ Nickel == Ni-Ni bonds

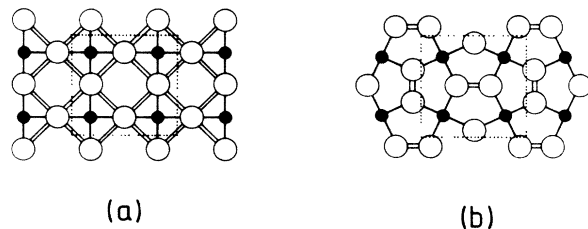


FIG. 1. Schematic representation of the carbon-induced reconstruction, showing the relevant interactions after chemisorption. The dotted line encloses the atoms included in the cluster of Fig. 2(b). (a) Unreconstructed surface indicating the positions of the adatoms for a $c(2 \times 2)$ structure. (b) Reconstructed surface.

Our *ab initio* study is based on total-energy calculations for small nickel clusters simulating a (001) surface. We employ the Kohn-Sham (KS) scheme⁹ with the local-density approximation (LDA) for exchange and correlation,¹⁰ and solve the one-electron problem in terms of localized muffin-tin-orbital basis functions,¹¹ including *s*, *p*, and *d* functions in all sites. The core electrons have been kept frozen, but all nickel *d* electrons have been explicitly incorporated in the calculations. For the low-coverage limit, we have utilized the cluster of Fig. 2(a), which consists of one adatom on a Ni₉ cluster, simulating the local environment of a fourfold hollow site. The calculated frequencies for the oscillation of the adatoms perpendicular to the surface are given by $\omega_{\perp}(\text{C}) = 430 \text{ cm}^{-1}$ and $\omega_{\perp}(\text{O}) = 400 \text{ cm}^{-1}$ for carbon and oxygen, respectively, in good agreement with the experimental values $\omega_{\perp}(\text{C}) = 410 \text{ cm}^{-1}$ and $\omega_{\perp}(\text{O}) = 400 \text{ cm}^{-1}$ for the low-coverage limit. For the equilibrium geometry we found $R_{\perp}(\text{C}) = 0.25 \text{ \AA}$ for carbon and $R_{\perp}(\text{O}) = 0.8 \text{ \AA}$ for oxygen, which compare well with the experimental values $R_{\perp}(\text{C}) = 0.2 \text{ \AA}$ and $R_{\perp}(\text{O}) = 0.88 \text{ \AA}$,¹² respectively. The binding energies are given by $E_b(\text{C}) = -11.4 \text{ eV}$ and $E_b(\text{O}) = -7.9 \text{ eV}$ for carbon and oxygen, respectively, although we recall that the local-density approximation tends to overestimate binding energies by about 15%.^{11,13}

For the case of 50% coverage we employed the cluster of Fig. 2(b), which consists of four adatoms on the same Ni₉ cluster used above. This cluster, which has been designed to represent the portion of the surface enclosed by the dotted line in Fig. 1, incorporates the main feature of *c*(2×2) structure, namely that each surface Ni atom is nearest-neighbor bonded to two adatoms. Keeping the position of the adatoms fixed at the bonding distances obtained from the low-coverage

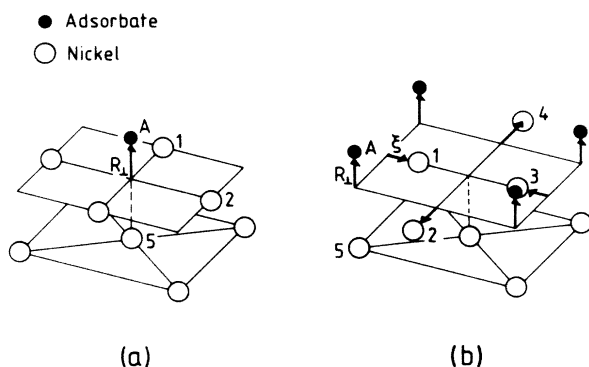


FIG. 2. (a) Cluster utilized for the low-coverage limit. Atom A is the adatom, located a distance R_{\perp} above the surface. Atoms 1–5 are Ni atoms referred to in the text. (b) Cluster utilized for the case of 50% coverage. The Ni atoms of the first metal layer are allowed to relax a distance ξ , to simulate a frozen A_2 phonon.

calculation, we have displaced the surface Ni atoms a distance ξ to simulate the frozen A_2 mode. While for oxygen the distortion is found to be energetically unfavorable, a finite distortion with $\xi = 0.53 \text{ \AA}$ lowers the energy of the cluster by 1.1 eV for carbon chemisorption.¹⁴ With the reconstruction the distance $R(1,3)$ shortens from the bulk second-neighbor value 3.52 to 2.47 \AA , i.e., it becomes shorter than the first-nearest-neighbor bulk distance, $a = 2.49 \text{ \AA}$, and the corresponding bond becomes stronger stabilizing the distorted structure; the distance $R(1,2)$ expands slightly to 2.60 \AA .

Various features of the orbital structure of the adatom-Ni₉ bond are the same in the oxygen and carbon cases. For instance, the adatom 2*s* level makes low-lying bonding and antibonding combinations with nickel 3*d* orbitals, which are both filled and have almost no net bonding effect. Also the interaction of the adatom 2*p* with the nickel 4*sp* orbitals is strictly bonding (the antibonding combinations are unoccupied) in both cases. On the other hand, the interaction between the adatom 2*p* and the nickel 3*d* orbitals exhibits marked differences. The corresponding bonding states are occupied in both cases but, while for carbon the antibonding states are empty, producing a large bonding, for oxygen most of them are occupied and produce net bonding contributions that are very small. The occupation of bonding and antibonding states gives rise to a closed-shell repulsion which prevents the oxygen from getting so close to the surface as the carbon does. In recent theoretical studies of oxygen chemisorption on nickel surfaces the *d* electrons have been treated by a pseudopotential, reducing nickel to a one-electron metal.^{3,4} Our results confirm that, provided one uses the correct occupation for the oxygen 2*p* levels, the neglect of the 2*p*_O-3*d*_{Ni} interaction should have little effect on the total energy. With the neglect of this interaction the O—Ni bond becomes rather sensitive to the occupation of the oxygen 2*p* levels, which now pin the Fermi level. This led Upton and Goddard to argue that the emptying of an oxygen 2*p* level could account for the softening of the vertical frequency of the frustrated translation of the O atom in *c*(2×2) overlayers.³ We find, on the contrary, that in the presence of nickel 3*d* electrons all bonding 2*p*_O levels lie more than 3 eV below E_F and that the O—Ni bond is actually quite insensitive to changes in the occupation numbers for levels near E_F , which are weakly bonding.

Because of the large binding energies one expects local changes in the metal-metal pair interactions to play an important role in the adatom-surface bonding. To describe these pair interactions we make use of standard population analysis, and introduce pair charges

$$Q(i,j) = \sum_{\alpha} Q_{\alpha}(i,j), \quad (1)$$

TABLE I. Equilibrium descreening and bonding charges for the clusters of Fig. 2. The Ni₉ cluster simulates the clean surface, the Ni₉A clusters (where A stands for O or C) simulate the low-coverage limit, and the Ni₉A₄ clusters simulate the case of 50% coverage.

	Ni ₉	Ni ₉ O	Ni ₉ O ₄	Ni ₉ C	Ni ₉ C ₄
$Q(A,A) - Z_c(A)$...	-0.16	0.02	-0.73	-0.58
$Q(1,1) - Z_c(1)$	-0.68	-0.74	-0.80	-0.68	-0.95
$Q(A,1)$...	0.30	0.23	0.53	0.58
$Q(A,5)$...	0.01	...	0.26	...
$Q(1,2)$	0.29	0.18	0.17	0.12	0.06
$Q(2,5)$	0.18	0.18	...	0.12	...

where

$$Q_\alpha(i,j) = 2 \sum_{L,L'} \langle \psi_\alpha | \chi_{i,L} \rangle \langle \chi_{i,L} | \chi_{j,L'} \rangle \langle \chi_{j,L'} | \psi_\alpha \rangle, \quad (2)$$

the summation \sum_α extends over all occupied states ψ_α , and the functions $\chi_{i,L}$, centered on the i th site with orbital symmetry $L = (l,m)$, have been taken to be localized muffin-tin orbitals. The off-diagonal terms $Q_\alpha(i,j)$ are positive (negative) for bonding (antibonding) states ψ_α and include only contributions due to the interference between orbitals centered on the i th and j th sites, so that the corresponding pair charge $Q(i,j)$ can be interpreted as the net bonding charge between these sites. The diagonal term $Q(i,i)$, which is positive definite, represents the amount of charge on the i th atom not involved in the bonding to other atoms, and provides the screening of its core charge $Z_c(i)$. In the following we shall loosely interpret the off-diagonal term $Q(i,j)$ as proportional to the orbital attraction between the i th and j th atoms, separated by a distance $R(i,j)$, and

$$[Q(i,i) - Z_c(i)][Q(j,j) - Z_c(j)]/R^2(i,j)$$

as the corresponding descreening repulsion.

The descreening and bonding charges of the clusters of Fig. 2, for oxygen and carbon chemisorption, are compared in Table I with those of the bare Ni₉ cluster. We notice the following: (i) The interaction between the adatom and the surface Ni atoms, as described by $Q(A,1)$, is stronger for carbon than for oxygen. (ii) The bonding charge $Q(A,5)$ shows that the C atom has an appreciable orbital interaction with the Ni atom 5 of the second metal layer, while the O atom does not. (iii) The bonding between the Ni atoms of the first and second layers, described by $Q(2,5)$ in Fig. 2(a), is somewhat weakened in the case of carbon, but shows no change for oxygen chemisorption. (iv) The Ni-Ni orbital interaction between the four adatom's nearest neighbors in the surface layer, described by $Q(1,2)$, is appreciably weakened by the chemisorption bond. The descreening repulsion between these atoms, $[Q(1,1) - Z_c(1)]^2/R^2(1,2)$, shows little change in the low-coverage case, but it is appreciably

increased in the case of 50% coverage. These two effects combine, giving rise to a net repulsive stress, which is stronger for larger coverage.

A lattice-dynamical model of the O-Ni(001) system should therefore allow for a nonvanishing first derivative of the pair potential between the surface Ni atoms, ϕ'_{11} (note that in such a model the net force on the surface Ni atoms still vanishes). A minimum set of force constants consistent with the *ab initio* results should, in addition, include a central force constant for the O-Ni coupling, ϕ''_{01} , and a central force constant for the coupling among the Ni atoms, which we take equal to the bulk value, $\phi''_b = 3.79 \times 10^4$ dyn/cm. We have studied the lattice dynamics of this model, using a fifteen-layer slab, whereby the matrix elements including stresses have been calculated according to standard methods (see, e.g., Ref. 7). We find that the inclusion of ϕ'_{11} does not affect the adsorbate modes, but has a dramatic influence on the substrate surface modes. The variation of the frequencies of the S_4 and the A_2 modes at \bar{X} are shown in Fig. 3 as a function of $\gamma = -\phi'_{11}/a\phi''_b$, where a is the first-nearest-neighbor Ni-Ni distance mentioned above. Both frequencies decrease with increasing γ , the effect being particularly pronounced for the A_2 mode. Since the A_2 mode is entirely localized within the first layer (in the nearest-neighbor model) its frequency can be written explicitly as

$$M_s \omega^2 = \phi''_b + 4\phi'_{11}/a, \quad (3)$$

where M_s is the mass of the surface atoms. This expression shows that the mode becomes soft for $\gamma = 0.25$. If one allows for second-neighbor interactions within the surface layer the mode may be stabilized for somewhat larger γ values. In order to obtain an estimate of the adsorbate-induced stresses for the $c(2 \times 2)$ structure, we evaluated the difference between the 1-2 bonding and descreening charges of the Ni₉A₄ (where A stands for C or O) and Ni₉ clusters, and assumed the bonding charge difference to be localized in the middle of the bond. A simple electrostatic calculation yields $\gamma \sim 0.16$ for oxygen and $\gamma \sim 0.4$ for carbon. Although these values should be taken only as very rough estimates, they strongly sug-

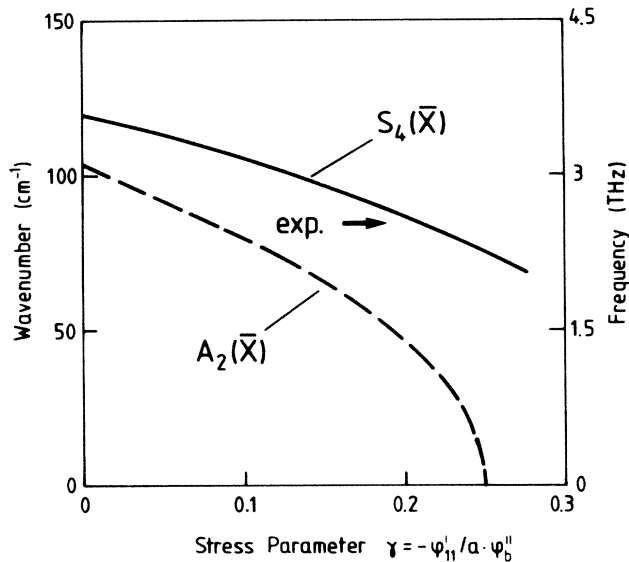


FIG. 3. Frequency variation of the S_4 and A_2 modes at the \bar{X} point of the surface Brillouin zone as a function of $\gamma = -\phi'_{11}/a\phi''_b$, for the $c(2 \times 2)$ oxygen-covered Ni(001) surface. The arrow points to the experimental value of the S_4 frequency for Ni(001) $c(2 \times 2)O$.²

gest that the difference between the behavior of oxygen and carbon on nickel surfaces lies in the strength of the induced surface stresses. Apparently, for carbon these stresses are able to drive the A_2 mode soft, while for oxygen they are not that strong, and they show up as a decrease of the frequency of the S_4 mode. For comparison, notice that the lattice-dynamical model requires $\gamma = 0.2$ to fit the experimental S_4 frequency at \bar{X} . (The observation of the A_2 mode is symmetry forbidden along $\bar{\Gamma}-\bar{X}$.)

Our results therefore show that adsorbate-induced lateral stresses between the surface atoms can explain the observed anomalously low frequency of the Rayleigh wave for the $c(2 \times 2)$ oxygen-covered surface and also the reconstruction observed with carbon (and nitrogen) overlayers. It is furthermore intuitively appealing to assume that for a clean surface ϕ'_{11} is positive (attractive), which would increase the frequency

of the Rayleigh wave beyond the value calculated with bulk data in agreement with experiment. We also note that ϕ'_{11}/a is equivalent to a macroscopic surface stress which, in absence of elastic waves, would give rise to capillary waves.¹⁵ Thus, the effect of ϕ'_{11}/a can be viewed as a capillary (or ripplon) contribution to the elastic surface waves.

The authors acknowledge many helpful discussions with Talat S. Rahman, and the critical reading of the manuscript by G. Comsa.

¹J. H. Onuferko, D. P. Woodruff, and B. W. Holland, *Surf. Sci.* **87**, 357 (1979).

²T. S. Rahman, D. L. Mills, J. E. Black, J. M. Seftel, S. Lehwald, and H. Ibach, *Phys. Rev. B* **30**, 589 (1984).

³T. H. Upton and W. A. Goddard, III, *Phys. Rev. Lett.* **46**, 1635 (1981).

⁴C. W. Bauschlicher, Jr., and P. S. Bagus, *Phys. Rev. Lett.* **52**, 200 (1984).

⁵W. Daum, to be published.

⁶H. Ibach, in *Festkörperprobleme: Advances in Solid State Physics*, edited by P. Grosse (Vieweg, Braunschweig, 1985), Vol. 25, p. 507.

⁷T. S. Rahman and H. Ibach, *Phys. Rev. Lett.* **54**, 1933 (1985).

⁸T. S. Rahman, M. Rocca, S. Lehwald, and H. Ibach, to be published.

⁹W. Kohn and L. J. Sham, *Phys. Rev.* **140**, A1133 (1965).

¹⁰We employed the parametrization of S. H. Vosko, L. Wilk, and M. Nussair, *Can. J. Phys.* **58**, 1200 (1980).

¹¹J. E. Müller, R. O. Jones, and J. Harris, *J. Chem. Phys.* **79**, 1874 (1983).

¹²J. Stöhr, R. Jaeger, and T. Kendelewicz, *Phys. Rev. Lett.* **49**, 142 (1982).

¹³Calculations on Ni_n-A clusters, for $n = 1, 2, 4, 5$, and 9, showed that total energies and bond distances have converged well at our cluster size.

¹⁴A smaller Ni_4C_4 cluster, including only the first layer of Ni atoms, exhibited the same reconstruction with an energy gain of 1.25 eV.

¹⁵See, for instance, L. D. Landau and E. M. Lifshitz, *Fluid Mechanics* (Pergamon, Oxford, 1959), Chap. 7.